

Metastable Charge Distribution Between Degenerate Landau Levels

Wenlu Lin,¹ Xing Fan,² Lili Zhao,¹ Yoon Jang Chung,³ Adbhut Gupta,³
Kirk W. Baldwin,³ Loren Pfeiffer,³ Hong Lu,^{2,4} and Yang Liu^{1,*}

¹International Center for Quantum Materials, Peking University, Haidian, Beijing 100871, China

²National Laboratory of Solid State Microstructures & Department of Materials Science and Engineering,
College of Engineering and Applied Sciences, Nanjing University, Nanjing 210093, China

³Department of Electrical Engineering, Princeton University, Princeton, New Jersey 08544, USA

⁴Shishan Laboratory, Suzhou Campus of Nanjing University, Suzhou 215000, China

(Dated: February 27, 2024)

We study two dimensional electron systems confined in wide quantum wells whose subband separation is comparable with the Zeeman energy. Two $N = 0$ Landau levels from different subbands and with opposite spins are pinned in energy when they cross each other and electrons can freely transfer between them. When the disorder is strong, we observe clear hysteresis in our data corresponding to instability of the electron distribution in the two crossing levels. When the intra-layer interaction dominates, multiple minima appear when a Landau level is $\frac{1}{3}$ or $\frac{2}{3}$ filled and fractional quantum hall effect can be stabilized.

I. INTRODUCTION

The quantum Hall effect is an incompressible quantum liquid phase signaled by the vanishing of the longitudinal conductance and the quantization of the Hall conductance seen in two-dimensional electron systems (2DES) at large perpendicular magnetic field [1, 2]. 2DES with spin and subband degree of freedom has additional sets of Landau levels (LLs) separated by the Zeeman energy E_Z or subband separation Δ_{SAS} , respectively [3–8]. When only a small number of LLs are occupied at LL filling factors $\nu < 4$, the electron distribution between the two subbands deviates from the $B = 0$ subband densities. The 2DES's Hartree potential leads to the renormalization of the subbands' energies and wavefunctions so that the total energy is minimized. When two LLs are degenerate at the Fermi energy, the electrons can redistribute between them with negligible energy cost [9–11].

High sensitivity, local capacitance measurement reveals fine structures and delicate quantum phases of the 2DES [12–20]. A recent examination by Lili Zhao *et al.* finds that the capacitance C and the conductance σ are

intertwined and both of them reflect the 2DES's transport properties [21]. In this work, we study the 2DES confined in wide quantum wells using the same technique as ref. 21 and discover features such as hysteresis and splitting minima, consistent with the pinning of two LLs and metastable charge distribution [22–24].

II. SAMPLES AND METHODS

We study two GaAs/AlGaAs samples grown by molecular beam epitaxy where the 2DESs are confined in the wide quantum wells and electrons occupy two subbands, leading to additional subband degree of freedom. We use back gate to change density and Δ_{SAS} increases when the charge distribution becomes imbalanced, see in Fig. 1(a). We study samples from two different wafers grown by different groups. The 45-nm-wide quantum well sample has 4.0 [25] as grown density and 6×10^4 cm²/(V·s) low temperature mobility and the 80-nm-wide quantum well sample has 1.1 as grown density and 6×10^6 cm²/(V·s) low temperature mobility. The Δ_{SAS} of the low mobility sample can be measured from the LL crossings seen when $\Delta_{SAS} = \hbar\omega_C$ and $\Delta_{SAS} = E_Z$, and the Δ_{SAS} of the high mobility sample can be extracted from the Fourier transform of the low field Shubnikov-de Hass oscillations. In both samples, Δ_{SAS} is comparable with the exchange-enhanced E_Z so that the S0 \downarrow and A0 \uparrow levels are close in energy (S and A refer to symmetric and antisymmetric subbands, 0 refers to the $N = 0$ LL index, \uparrow and \downarrow refer to up- and down-spin) [26–28]. Although the subband wavefunctions are not strictly symmetric or antisymmetric when charge distribution is imbalanced, for simplicity, we still use S and AS for the two subbands.

Each sample is a 2×2 mm² cleaved piece, with eight alloyed InSn contacts; see the Fig. 1(b). We fit the samples with an In back gate to tune the electron density, and evaporate multiple Ti/Au front gates with Corbino-like geometry for capacitance measurement. The outer radius of G1 and the inner radius of G2 are $r_1 = 120$

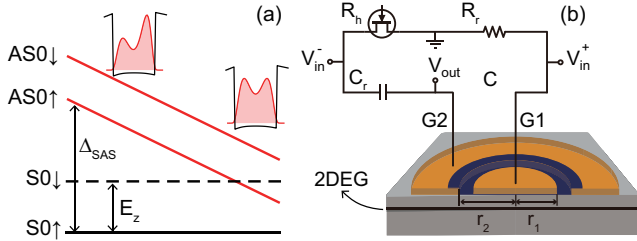


FIG. 1. (a) Relevant energy levels and charge distribution in wide quantum well. (b) Schematic of gates with Corbino-like geometry for capacitance measurements.

* liuyang02@pku.edu.cn

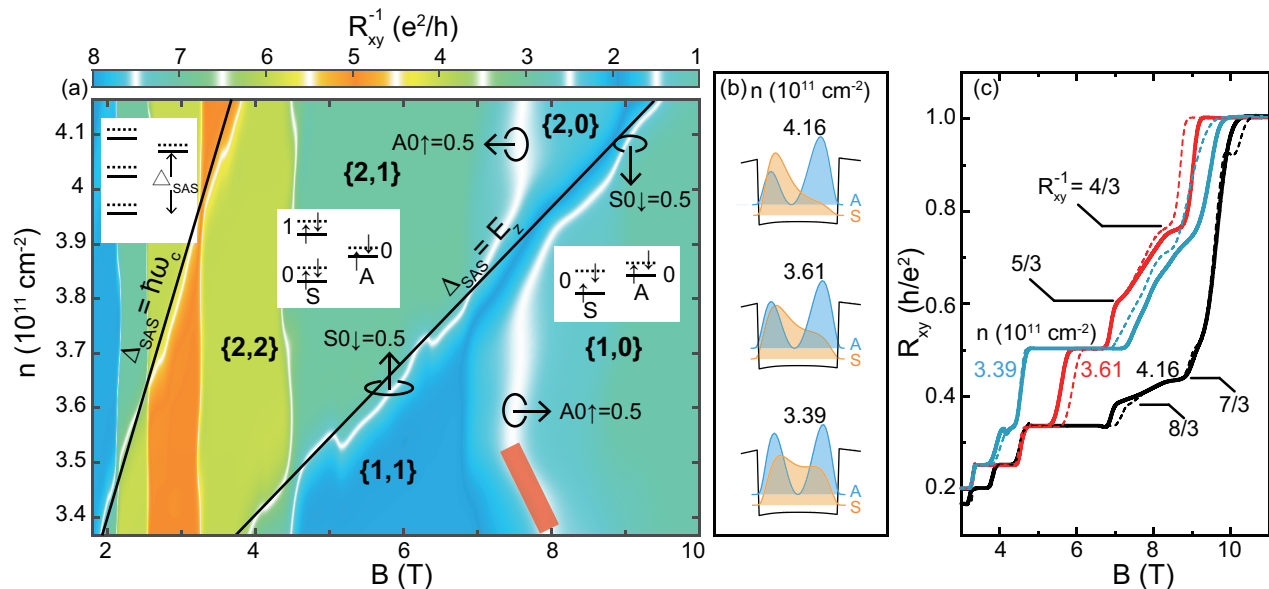


FIG. 2. (a) Color-coded plot of R_{xy}^{-1} as a function of n and B . The insets are LL diagrams corresponding to three regions separated by the $\Delta_{SAS} = \hbar\omega_c$ and $\Delta_{SAS} = E_z$ lines. Plaques with different colors correspond to different R_{xy} plateaus, where $\{\nu_S, \nu_A\}$ labels the number of LLs belong to the two subbands whose electron filling factor is higher than 1/2. (b) Calculated charge distribution ($|\psi_S|^2$ and $|\psi_A|^2$) for the two subbands of 45-nm-wide quantum well sample at different n . (c) R_{xy} vs. B traces at different n . We use solid and dashed traces for up- and down-sweep respectively in all figures throughout this manuscript.

μm and $r_2 = 140 \mu\text{m}$, respectively; see the Fig. 1(b). Capacitance is measured between the two gates using a cryogenic bridge and excitation frequency up to 140 MHz [29]. The capacitance (C) and conductance (G) components can be extracted from the in-phase and out-of-phase of the bridge output V_{out} [30]. The longitudinal and Hall resistances, R_{xx} and R_{xy} , can be measured *in-situ* using standard lock-in technique (< 40 Hz). All the experiments are performed in a dilution refrigerator whose base temperature is 10 mK.

III. RESULTS AND DISCUSSION

Fig. 2(a) shows the color-coded plot of R_{xy}^{-1} as a function of magnetic field B and electron density n , taken from the 45-nm-wide quantum well sample. In Fig. 2(a), colored plaques represent different quantized Hall conductances $\sigma_{xy} = R_{xy}^{-1}$ where $R_{xx} = 0$, and plateau-to-plateau transitions appears as white ribbons. This sample has low mobility so that the disorder dominates and each Landau level contributes zero/one Hall conductance [25] if its filling factor is below/above 1/2, respectively. The plateau-to-plateau transitions appear when a LL is exactly half filled.

We highlight two series of transitions by the two black lines which correspond to the conditions $\Delta_{SAS} = \hbar\omega_c$ and $\Delta_{SAS} = E_z$ as labeled in Fig. 2(a) [4, 31]. The charge distribution is balanced when $n \simeq 3.0$ and the higher density leads to a more imbalanced quantum well

[25]. Δ_{SAS} increases from about 40 to 80 K as n increases from 3.4 to 4.1, deduced from the $\Delta_{SAS} = \hbar\omega_c$ line [4]. The $\Delta_{SAS} = E_z$ line appears at about twice the magnetic field than the $\Delta_{SAS} = \hbar\omega_c$ line, suggesting that E_z is significantly enhanced by about 30 times because of the exchange energy [26–28]. These two lines separate Fig. 2(a) into three zones with different LL configurations shown by the insets. We label the number of more-than-half-filled LLs from the symmetric and anti-symmetric subbands as $\{\nu_S, \nu_A\}$ for each colored plaque in Fig. 2(a) [4, 8, 31].

It is quite surprising that the $\{1,0\}$ -to- $\{1,1\}$ boundary, at which the $A0\uparrow$ level is half-filled, moves towards lower field while the total density increases, see the thick red line. This anomalous phenomenon can be better illustrated by Fig. 2(c), where the R_{xy} of the $n = 3.61$ trace is larger than the $n = 3.39$ trace at $B \gtrsim 6$ T. The kink at $R_{xy} = 3/5$ and $3/4$ [25] in the $n = 3.61$ trace signals the formation of fractional quantum Hall effect when the $A0\uparrow$ is $1/3$ and $2/3$ filled, respectively. According to the total filling factor, the $S0\downarrow$ level is less-than-half filled at about 0.4 and contributes zero Hall conductance. On the $\{2,0\}$ -to- $\{2,1\}$ boundary, the R_{xy} trace at $n = 4.16$ exhibits kinks at $R_{xy} = 3/7$ and $3/8$ at similar B , signaling that the $A0\uparrow$ is $1/3$ and $2/3$ filled when the $S0\downarrow$ level is more-than-half filled at about 0.7 and contributes e^2/h in Hall conductance. The above observations suggest that the $S0\downarrow$ and $A0\uparrow$ levels are both partially filled and energetically degenerate at the Fermi energy in a large range of B and n , i.e. the two crossing LLs are pinned together

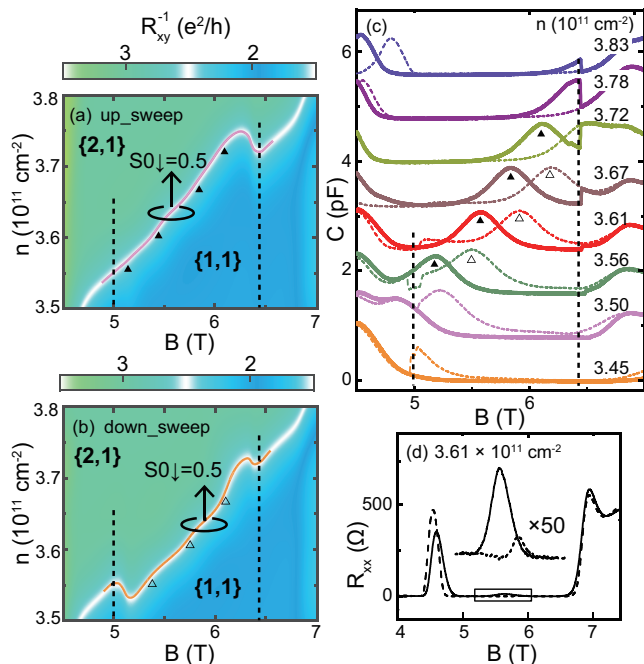


FIG. 3. (a, b) Color-coded plot of R_{xy}^{-1} as a function of n and B near the $\{1,1\}$ -to- $\{2,1\}$ boundary of the up- and down-sweep data respectively. The pink and orange lines highlight the positions of plateau-to-plateau transition where clear hysteresis appears. (c) C vs B traces at different n . We mark the C peak in the up- and down-sweep data and summarize their positions in panel (a, b) with solid and open symbols, respectively. (d) R_{xx} vs. B trace of density $3.61 \times 10^{11} \text{ cm}^{-2}$, and inset shows hysteresis after 50 times magnification.

and both of them will be partially occupied in a finite range of B and n [9–11, 32, 33].

Hysteresis occurring at the $\{1,1\}$ -to- $\{2,1\}$ boundary is shown in Fig. 3(a) and 3(b), across which the filling factor of the $S0\downarrow$ level varies through $1/2$, see also the $n = 3.61$ data near 6 T in Fig. 2(c). This hysteresis can be better seen in Fig. 3(c). The capacitance C vanishes when the system forms a quantum Hall effect and a peak appears whenever a LL is exactly half-filled [21]. More specifically, the peaks in the up- and down-sweep traces, where the $S0\downarrow$ level is half filled, appear at different fields. We mark the capacitance peak seen in the up- and down-sweep traces and summarize their positions in Fig. 3(a) and Fig. 3(b) with solid and open symbols, respectively. The hysteresis, i.e. the peak position depends on the sweep direction, indicating a metastable charge distribution in the two energetically locked LLs. The sharp capacitance jumps near the dashed lines mark the onset of the discrepancy between the up- and down-sweeps, possibly due to the completely emptying or filling of the $A0\uparrow$ level [34]. We also show transport results in Fig. 3(d) at $n = 3.61$ where a barely visible R_{xx} peak appears at the $\{1,1\}$ -to- $\{2,1\}$ boundary and a hysteresis behavior is also seen, consistent with previous reports [35–37]. The R_{xx} peak is a narrow spike appearing only at the

boundary when one LL is exactly half-filled, while the hysteresis region in our capacitance data is much broader with two sharp ends far from the boundary, see the two dashed lines in Fig. 3(d). This is because our capacitance measurement is a local probe achieved by gates without contacts involved, so that it is sensitive to local domains and charge instability caused by LL pinning and domains. The transport measurement, on the other hand, averages across the whole sample and the domains can be seen only when they form a percolation network at the plateau-to-plateau transition boundary. Therefore, we can observe hysteretic behavior in C measurements while the transport features are barely visible.

The charge transfer is universally present in imbalanced 2DES confined in wide and double quantum wells [10, 11]. Empirically, visible hysteresis phenomena are usually seen strong when the 2DES forms strong insulating phases so that the time constant for charge transfer is sufficiently long [23, 24]. It is also seen if domain structure forms when two LLs with different spins cross [35–37]. In general, the random disorder plays an essential role in the hysteresis. We study the low-disorder 80-nm-wide quantum well sample below. The low-field subband separation Δ_{SAS} measured from the Fourier transform of the Shubnikov-de Haas oscillations is shown in the Fig. 4(b). It increases from 10 K to about 17 K when we reduce n from 1.3 to 0.88 by back-gate voltage. In Fig. 4(a), the R_{xx} minimum at $\nu = 8/3$ disappears in the $n=1.1$ trace signaling that Δ_{SAS} equals E_Z which is ~ 23 -times enhanced [28]. In the high mobility samples, disorder is reduced so that the electron-electron interaction stabilizes fractional quantum Hall states. Fractional quantum Hall effects can be understood as integer quantum Hall effects of composite fermion which forms by attaching 2 flux quanta to each particle [38]. Fractional quantum Hall state at $\nu = 8/3$ is $\nu = 1/3$ of holes and is stable when either $\Delta_{SAS} > E_Z$ or $\Delta_{SAS} < E_Z$; see in Fig. 4(c). It disappears if and only if $S0\downarrow$ and $A0\uparrow$ are degenerate and the disappearance of minima at $\nu = 8/3$ signals the exact condition $\Delta_{SAS} = E_Z$ [28]. Similarly, a weakening of the $\nu = 4/3$ and $7/5$ states is also visible, suggesting that the $S0\downarrow$ and $A0\uparrow$ levels are close in energy within the B and n range of our study. In the capacitance trace, hysteresis is only seen near the integer filling factors $\nu = 1$ and 2 , where the 2DES consists of incompressible quantum Hall effect and randomly pinned quasiparticles/quasiholes [34]. This hysteresis gradually disappears at high temperatures above 400 mK when the thermal fluctuation softens the disorder pinning, see Fig. 5(a) and (b). It's also quite possible that these dilute quasiparticles/quasiholes may form a Wigner crystal which has a large capacitance response [30]. In Fig. 5(c), we show R_{xx} at base temperature and 208 mK where no hysteresis at any temperature is seen. This is consistent with Fig. 3 results: C is sensitive to local domain while R_{xx} is an average over the entire sample, so that C can reflect local charge transfer between subbands.

When the partial filling factor in the LLs increases, the

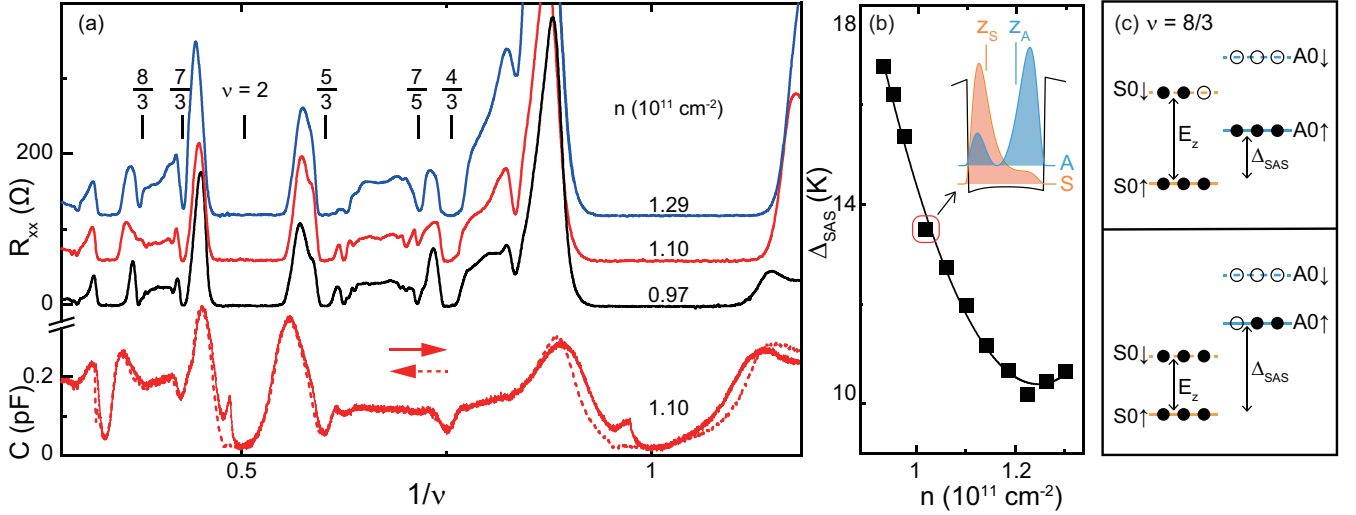


FIG. 4. (a) The longitudinal resistance (R_{xx}) and capacitance (C) taken from the 80-nm-wide quantum well sample. Hysteresis of C can be observed within the R_{xx} plateau region at integer quantum Hall effects. (b) The experimentally measured low field Δ_{SAS} deduced from the Shubnikov–de Haas oscillation. We also show calculated charge distribution ($|\psi_S|^2$ and $|\psi_A|^2$) for the two subbands, and the vertical bars label z_S and z_A mark their centroid $\langle \psi | \hat{z} | \psi \rangle$. (c) Diagram shows the two configurations for stable $\nu = 8/3$ fractional quantum Hall states in two-subband picture. The electrons and holes are marked as solid and open circles, respectively. We use red and blue lines to distinguish symmetric and antisymmetric subband.

electron interaction stabilizes fractional quantum Hall effects and the hysteresis disappears. We can deduce the local conductance G between the two Corbino-like gates [21], see Fig. 6(a). The two subbands can be understood as parallel channels. R_{xx} shows minima only if two subbands are both insulating, so that the R_{xx} minima only appear at specific $\nu = 7/3$ and $8/3$, etc. The measured C is the sum of these two parallel channels so that minima can be observed whenever one LL has $\frac{1}{3}$ or $\frac{2}{3}$ insulating states in Fig. 6(a). At $n=1.1$, no minima is seen for the $\nu = 8/3$ state when the two configurations $(\nu_{S0\downarrow}, \nu_{A0\uparrow}) = (\frac{2}{3}, 1)$ and $(1, \frac{2}{3})$ have the same energy, which is consistent with R_{xx} results in Fig. 4(a); $\nu_{S0\downarrow}$ and $\nu_{A0\uparrow}$ are the corresponding filling factor of the $S0\downarrow$ and $A0\uparrow$ levels [28]. Δ_{SAS} increases as n decreases so that the $S0\downarrow$ level becomes more populated and the $(1, \frac{2}{3})$ configuration is energetically favorable. However, the subbands of asymmetric quantum well has different z_S and z_A , the center of their charge distribution $\langle \psi | \hat{z} | \psi \rangle$, which leads to finite energy cost for redistributing electrons between them, see Fig. 4(b). Therefore the in-plane Coulomb interaction can no longer stabilize the $8/3$ state at exact total filling factor. Instead, a minimum reappears but shifts to smaller filling factors, corresponding to $(1-\nu^*, \frac{2}{3})$ where some quasiholes (ν^*) appear in the $S0\downarrow$ level. Meanwhile, the $7/3$ state has the configuration $(\frac{2}{3}, \frac{2}{3})$ when the $S0\downarrow$ and $A0\uparrow$ levels are degenerate at $n=1.26$ so that a single minimum appears at exactly $7/3$ total filling factor. When the energy of $A0\uparrow$ level increases at $n \leq 1.26$, this minimum splits into two at which the system has configuration of $(\frac{2}{3}+\nu^*, \frac{2}{3})$ and $(\frac{2}{3}, \frac{2}{3}-\nu^*)$, respectively [39].

We summarize the quasi-particle or quasi-hole densi-

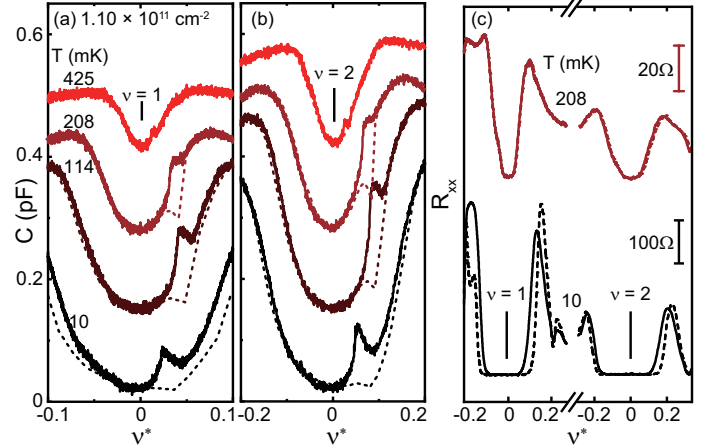


FIG. 5. (a, b) The hysteresis of C around $\nu = 1$ and 2 gradually disappears as temperature increases to $\gtrsim 400$ mK. (c) R_{xx} results at base temperature and 208 mK.

ties, $n^* = n \cdot \nu^* / \nu$, for several observed G minima in Fig. 6(b). We note that the hysteresis near $\nu = 2$ in Fig. 6(a) also has a density dependent evolution, where the peak in the up-sweep gradually shifts to higher filling as n decreases. It is likely that this peak signals the formation of the integer quantum Hall effect by spontaneously fill up the $A0\uparrow$ level [34]. The residual quasiparticle density n^* in the $S0\downarrow$ level increases when the density decreases, which generates a Hartree potential to compensate the increasing Δ_{SAS} . For example, $n^* = 0.02$ reduces the antisymmetric subband energy by $\simeq e^2 n^* / \epsilon |z_S - z_A| \simeq 10$ K, where e is the electron charge, ϵ is the GaAs perm-

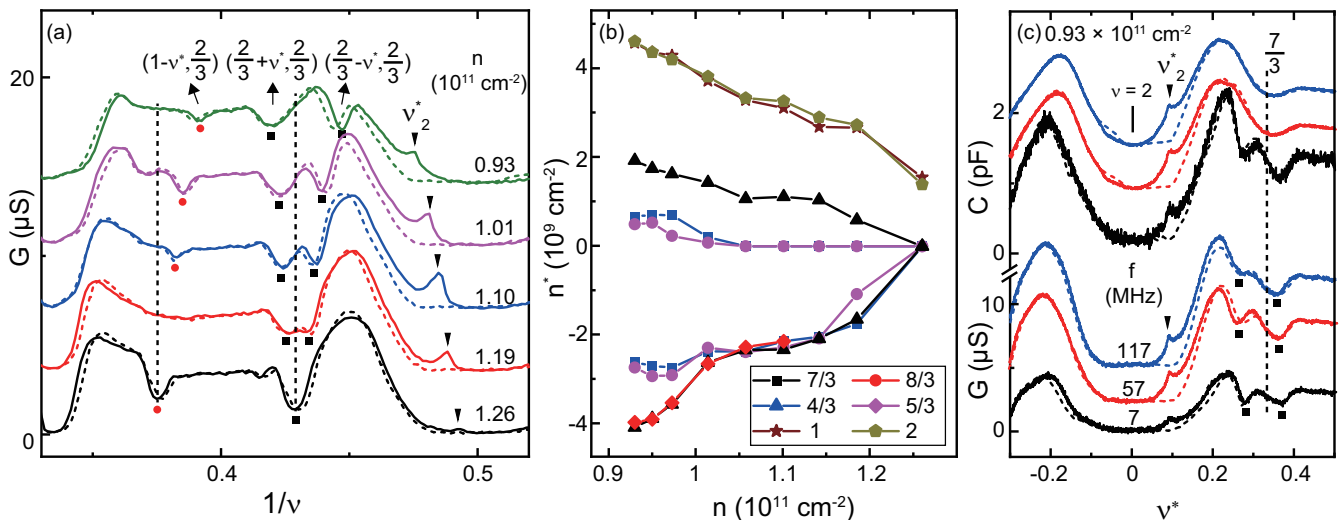


FIG. 6. (a) Local conductance component extracted from the capacitance measurements. Data taken from the 80-nm-wide quantum well sample at different densities. We mark hysteresis and double minima with different symbols to illustrate their evolution as a function of quantum well symmetry. ($\nu_{S0\downarrow}, \nu_{A0\uparrow}$) signals LL configuration, and we also use ν^* to mark the filling location of the maximal hysteresis of integer quantum Hall effect. (b) Summary of quasi-particle and quasi-hole densities of different features. (c) Local conductance and capacitance measured by using different frequencies.

tivity and $|z_S - z_A| \simeq 31 \text{ nm}$ is the equivalent charge separation between the two subbands (see Fig. 4(b)). We also summarize the density of residual charges near $\nu=1$ and 2 in Fig. 6(b).

Fig. 6(c) studies the split minima near $7/3$ and the hysteresis near $\nu = 2$ as a function of measurement frequency f . The hysteresis around $\nu = 2$ becomes more profound at higher frequencies both in C and G , consistent with the assumption that it's the response of pinned charges. On the other hand, the split minima around $7/3$ is a low-frequency phenomenon, i.e. the G minima becomes shallower at high frequencies, and only one shallow minimum at $7/3$ appears in the capacitance at $f = 57$ and 117 MHz. This may be because that the dilute extra quasiparticles/quasiholes can response to the probing high frequency electric field and screen the minima.

IV. CONCLUSION

In summary, we closely examine the 2DES confined in wide quantum wells using capacitance measurement. Our results indicate that the $S0\downarrow$ and $A0\uparrow$ levels are pinned in energy if the subband separation and exchange-enhanced Zeeman energy are comparable. We discover hysteresis and charge instability when the disorder is strong, and multiple minima at fractional quantum Hall effect if the intra-layer interaction dominates. Our observations shed light on the complex internal structure of 2DES when multiple degrees of freedom present.

ACKNOWLEDGMENTS

We acknowledge support by the National Natural Science Foundation of China (Grant No. 92065104 and 12074010) and the National Basic Research Program of China (Grant No. 2019YFA0308403) for sample fabrication and measurement. This research is funded in part by the Gordon and Betty Moore Foundation's EPiQS Initiative, Grant GBMF9615 to L. N. Pfeiffer, and by the National Science Foundation MRSEC grant DMR 2011750 to Princeton University. We thank L. W. Engel, Bo Yang and Xi Lin for valuable discussion.

- [1] D. C. Tsui, H. L. Stormer, and A. C. Gossard, Two-dimensional magnetotransport in the extreme quantum limit, *Phys. Rev. Lett.* **48**, 1559 (1982).
 [2] K. v. Klitzing, G. Dorda, and M. Pepper, New method for high-accuracy determination of the fine-structure constant based on quantized hall resistance,

Phys. Rev. Lett. **45**, 494 (1980).

- [3] N. Kumada, K. Iwata, K. Tagashira, Y. Shimoda, K. Muraki, Y. Hirayama, and A. Sawada, Modulation of bilayer quantum hall states by tilted-field-induced subband-landau-level coupling, *Phys. Rev. B* **77**, 155324 (2008).

- [4] Y. Liu, J. Shabani, and M. Shayegan, Stability of the $q/3$ fractional quantum hall states, *Phys. Rev. B* **84**, 195303 (2011).
- [5] D. Zhang, S. Schmult, V. Venkatachalam, W. Dietsche, A. Yacoby, K. von Klitzing, and J. Smet, Local compressibility measurement of the $\nu_{tot} = 1$ quantum hall state in a bilayer electron system, *Phys. Rev. B* **87**, 205304 (2013).
- [6] X. Liu, Z. Hao, K. Watanabe, T. Taniguchi, B. I. Halperin, and P. Kim, Interlayer fractional quantum hall effect in a coupled graphene double layer, *Nature Physics* **15**, 893 (2019).
- [7] J. I. A. Li, Q. Shi, Y. Zeng, K. Watanabe, T. Taniguchi, J. Hone, and C. R. Dean, Pairing states of composite fermions in double-layer graphene, *Nature Physics* **15**, 898 (2019).
- [8] Q. Shi, E.-M. Shih, D. Rhodes, B. Kim, K. Barmak, K. Watanabe, T. Taniguchi, Z. Papić, D. A. Abanin, J. Hone, and C. R. Dean, Bilayer wse2 as a natural platform for interlayer exciton condensates in the strong coupling limit, *Nature Nanotechnology* **17**, 577 (2022).
- [9] S. Trott, G. Paasch, G. Gobsch, and M. Trott, Magnetic-field-dependent self-consistent electronic structure of an inversion layer in the two-subband state, *Phys. Rev. B* **39**, 10232 (1989).
- [10] Y. Liu, J. Shabani, D. Kamburov, M. Shayegan, L. N. Pfeiffer, K. W. West, and K. W. Baldwin, Evolution of the $7/2$ fractional quantum hall state in two-subband systems, *Phys. Rev. Lett.* **107**, 266802 (2011).
- [11] J. Nuebler, B. Friess, V. Umansky, B. Rosenow, M. Heiblum, K. von Klitzing, and J. Smet, Quantized $\nu = 5/2$ state in a two-subband quantum hall system, *Phys. Rev. Lett.* **108**, 046804 (2012).
- [12] V. Mosser, D. Weiss, K. Klitzing, K. Ploog, and G. Weimann, Density of states of gaas-algaas-heterostructures deduced from temperature dependent magnetocapacitance measurements, *Solid State Communications* **58**, 5 (1986).
- [13] T. P. Smith, W. I. Wang, and P. J. Stiles, Two-dimensional density of states in the extreme quantum limit, *Phys. Rev. B* **34**, 2995 (1986).
- [14] R. C. Ashoori, H. L. Stormer, J. S. Weiner, L. N. Pfeiffer, S. J. Pearton, K. W. Baldwin, and K. W. West, Single-electron capacitance spectroscopy of discrete quantum levels, *Phys. Rev. Lett.* **68**, 3088 (1992).
- [15] J. P. Eisenstein, L. N. Pfeiffer, and K. W. West, Negative compressibility of interacting two-dimensional electron and quasiparticle gases, *Phys. Rev. Lett.* **68**, 674 (1992).
- [16] A. A. Zibrov, C. Kometter, H. Zhou, E. M. Spanton, T. Taniguchi, K. Watanabe, M. P. Zaletel, and A. F. Young, Tunable interacting composite fermion phases in a half-filled bilayer-graphene landau level, *Nature* **549**, 360 (2017).
- [17] H. Irie, T. Akiho, and K. Muraki, Determination of g-factor in InAs two-dimensional electron system by capacitance spectroscopy, *Applied Physics Express* **12**, 063004 (2019).
- [18] Q. Shi, E.-M. Shih, M. V. Gustafsson, D. A. Rhodes, B. Kim, K. Watanabe, T. Taniguchi, Z. Papić, J. Hone, and C. R. Dean, Odd- and even-denominator fractional quantum hall states in monolayer wse2, *Nature Nanotechnology* **15**, 569 (2020).
- [19] H. Deng, L. N. Pfeiffer, K. W. West, K. W. Baldwin, L. W. Engel, and M. Shayegan, Probing the melting of a two-dimensional quantum wigner crystal via its screening efficiency, *Phys. Rev. Lett.* **122**, 116601 (2019).
- [20] S. L. Tomarken, Y. Cao, A. Demir, K. Watanabe, T. Taniguchi, P. Jarillo-Herrero, and R. C. Ashoori, Electronic compressibility of magic-angle graphene superlattices, *Phys. Rev. Lett.* **123**, 046601 (2019).
- [21] L. Zhao, W. Lin, Y. J. Chung, K. W. Baldwin, L. N. Pfeiffer, and Y. Liu, Finite capacitive response at the quantum hall plateau, *Chinese Physics Letters* **39**, 097301 (2022).
- [22] J. Pollanen, J. P. Eisenstein, L. N. Pfeiffer, and K. W. West, Charge metastability and hysteresis in the quantum hall regime, *Phys. Rev. B* **94**, 245440 (2016).
- [23] E. Tutuc, R. Pillarisetty, S. Melinte, E. P. De Poortere, and M. Shayegan, Layer-charge instability in unbalanced bilayer systems in the quantum hall regime, *Phys. Rev. B* **68**, 201308 (2003).
- [24] H. Deng, Y. Liu, I. Jo, L. N. Pfeiffer, K. W. West, K. W. Baldwin, and M. Shayegan, Interaction-induced interlayer charge transfer in the extreme quantum limit, *Phys. Rev. B* **96**, 081102 (2017).
- [25] We omit the unit of the charge density 10^{11} cm^{-2} and the unit of the conductance (resistance) e^2/h (h/e^2) throughout this manuscript for brevity.
- [26] K. Muraki, T. Saku, and Y. Hirayama, Charge excitations in easy-axis and easy-plane quantum hall ferromagnets, *Phys. Rev. Lett.* **87**, 196801 (2001).
- [27] X. C. Zhang, I. Martin, and H. W. Jiang, Landau level anticrossing manifestations in the phase-diagram topology of a two-subband system, *Phys. Rev. B* **74**, 073301 (2006).
- [28] Y. Liu, S. Hasdemir, J. Shabani, M. Shayegan, L. N. Pfeiffer, K. W. West, and K. W. Baldwin, Multicomponent fractional quantum hall states with subband and spin degrees of freedom, *Phys. Rev. B* **92**, 201101 (2015).
- [29] L. Zhao, W. Lin, X. Fan, Y. Song, H. Lu, and Y. Liu, High precision, low excitation capacitance measurement methods from 10 mk to room temperature, *Review of Scientific Instruments* **93**, 053910 (2022).
- [30] L. Zhao, W. Lin, Y. J. Chung, A. Gupta, K. W. Baldwin, L. N. Pfeiffer, and Y. Liu, Dynamic response of wigner crystals, *Phys. Rev. Lett.* **130**, 246401 (2023).
- [31] J. Falson, D. Maryenko, B. Friess, D. Zhang, Y. Kozuka, A. Tsukazaki, J. H. Smet, and M. Kawasaki, Even-denominator fractional quantum hall physics in zno, *Nature Physics* **11**, 347 (2015).
- [32] C. H. W. Barnes, A. G. Davies, K. R. Zolleis, M. Y. Simmons, and D. A. Ritchie, Intrinsic coupling mechanisms between two-dimensional electron systems in double quantum well structures, *Phys. Rev. B* **59**, 7669 (1999).
- [33] V. M. Kaganer, B. Jenichen, F. Schippan, W. Braun, L. Däweritz, and K. H. Ploog, Strain-mediated phase coexistence in mnas heteroepitaxial films on gaas: An x-ray diffraction study, *Phys. Rev. B* **66**, 045305 (2002).
- [34] J. Zhu, H. L. Stormer, L. N. Pfeiffer, K. W. Baldwin, and K. W. West, Hysteresis and spikes in the quantum hall effect, *Phys. Rev. B* **61**, R13361 (2000).
- [35] E. P. De Poortere, E. Tutuc, and M. Shayegan, Critical resistance in the alas quantum hall ferromagnet, *Phys. Rev. Lett.* **91**, 216802 (2003).
- [36] W. Pan, J. L. Reno, and J. A. Simmons, Hysteresis in the quantum hall regimes in electron double quantum well structures, *Phys. Rev. B* **71**, 153307 (2005).

- [37] V. Piazza, V. Pellegrini, F. Beltram, W. Wegscheider, T. Jungwirth, and A. H. MacDonald, First-order phase transitions in a quantum hall ferromagnet, *Nature* **402**, 638 (1999).
- [38] J. K. Jain, *Composite Fermions* (Cambridge University Press, Cambridge, UK, 2007).
- [39] We would like to emphasize that in quasi-DC transport we always observe minimum at proper total filling factors in Fig. 4(a). A more comprehensive study is necessary to explain the discrepancy.